Final report on the EOS validation investigation: Surface Radiation Budget and Cloud Measurements for NASA's EOS CERES Program

John Augustine and Chuck Long
May 7, 2003

Objectives

The objective of this investigation is to provide SURFRAD network data and special research-supporting ancillary products for validation of the CERES instruments aboard EOS satellites TRMM, Terra, and Aqua. This final year of funding covered only a half-year. Our goals were:

1) Install a new SURFRAD station
2) Improve Total Sky Imager (TSI) processing and reprocess all TSI data
3) Continue to provide clear-sky identification files and other data to EOS investigators
4) Develop a method to estimate infrared cloud forcing at the surface
5) Improve the interpolated soundings

Accomplishments

New SURFRAD station

Although new stations are not a part of this EOS contract, we strive to continue to add new sites in different climates to enhance the value of SURFRAD to climate research and EOS and NESDIS validation efforts. During 2002 the opportunity arose to add a station at the Canaan Valley in northern West Virginia. The land where the new site is to be located is owned and managed by the Dept. of Interior Fish and Wildlife Service. Unfortunately, they have deferred lease negotiations with NOAA in lieu of more pressing matters. Given the delay, attention turned to adding a new station at the EROS Data Center near Sioux Falls, SD. A lease has been obtained with the USGS and the new SURFRAD station is scheduled to be installed in June 2003. It will be collocated with a USGS SCAN (soil moisture) site, a GPS water vapor CORS station, a CRN station, and an EOS/MODIS antenna.

TSI topics

Optimize TSI settings at all SURFRAD locations

Each TSI must be optimized through a variety of settings to compensate for the conditions in which it operates as well as for slight differences in the characteristics of the individual cameras. The first is the brightness setting of the camera, which defines the "lightness" or "darkness" of the sky images. The second designates the size of regions for masking sun glint around the solar disk and the horizon. The third controls the sensitivity to distinguish between thin and opaque clouds and between thin cloud and clear sky. Setting up a TSI is an iterative process that requires assigning these parameters, watching images, and making adjustments as necessary. This process must be repeated until the operators are satisfied with the cloud definitions and the computations of hemispheric fractional cloud cover. The camera brightness is the only non-recoverable setting; changes in the others are implemented simply by reprocessing the data.

Upon viewing the products from all TSIs for several weeks, it was determined that the camera brightness levels should be set uniformly to 6. Changing the brightness parameter

from 5 to 6 significantly improved the Desert Rock TSI products, but the common occurrence of cirrus clouds there continued to cause high TSI biases. This was remedied by adjusting the cloud definition thresholds, which affect the sensitivities to thin cloud, opaque cloud, and clear sky. Similar problems were encountered with Fort Peck TSI and the appropriate adjustments were made. The threshold settings were only slightly adjusted for the other stations. After the optimum settings were determined for all SURFRAD TSIs, their data were reprocessed.

Access the performance of the TSI in determining cloud fraction

The most important information that the TSIs provide to EOS investigators is a ground-based measure of cloud fraction. However, a careful comparison of TSI cloud fractions to subjective observations made by trained weather observers has never been done. Because of the proliferation of ASOS stations at NWS sites the opportunities for these comparisons are diminishing. Fortunately, the Desert Rock SURFRAD site is collocated with an upper air station where hourly cloud cover observations continue to be made.

Trained NWS observers "bin" their perception of cloud cover into octaves and convert their observations to cloud fraction in eights. Therefore, to make valid comparisons between TSI cloud fractions and observer-estimated cloud cover, the TSI cloud fraction had to be converted to eighths. Because the TSI can, for a variety of reasons, report small amounts of “phantom” clouds under clear sky conditions, it was decided to set the threshold for "clear" conditions (0/8) at TSI cloud fractions ≤ 2%. NWS observers record 8/8 sky cover only when the sky is overcast. Accordingly, only TSI reports of 100% cloud cover are binned as 8/8. The other TSI cloud-cover percentages (3 to 99%) were assigned into bins corresponding to eighths of the hemispheric sky.

Differences between the TSI and observer-determined sky cover were calculated for each observation time. The differences were then put in one of 17 bins (-8 to 8) and plotted as a percentage of the total. This procedure was followed for those times when, according to the observer, no cirrus clouds of any type were present (version 1) and for those times when only cirrus clouds were present (version 2). Separating the dataset in this manner allowed a first order determination of the effectiveness of the TSI at identifying thin and opaque clouds separately.

For version 1 (Figure 1), ninety percent of the differences are ±1 octave, of which 62% are in the zero bin, i.e., no difference between the TSI and observers. With this sharp, near normal distribution centered on zero, it can be concluded that the TSI gives good results when clouds are opaque. However, when only cirrus clouds are present (according to the observer), the differences are almost exclusively negative (not shown). This suggests that there is a sensitivity difference in what the observer and the TSI tend to set as the clear-thin cloud threshold. If the TSI is adjusted to identify more of the thin cirrus clouds, it will falsely identify opaque clouds and thus misrepresent the true cloud fraction. Details of this work are presented in Hodges (2003).

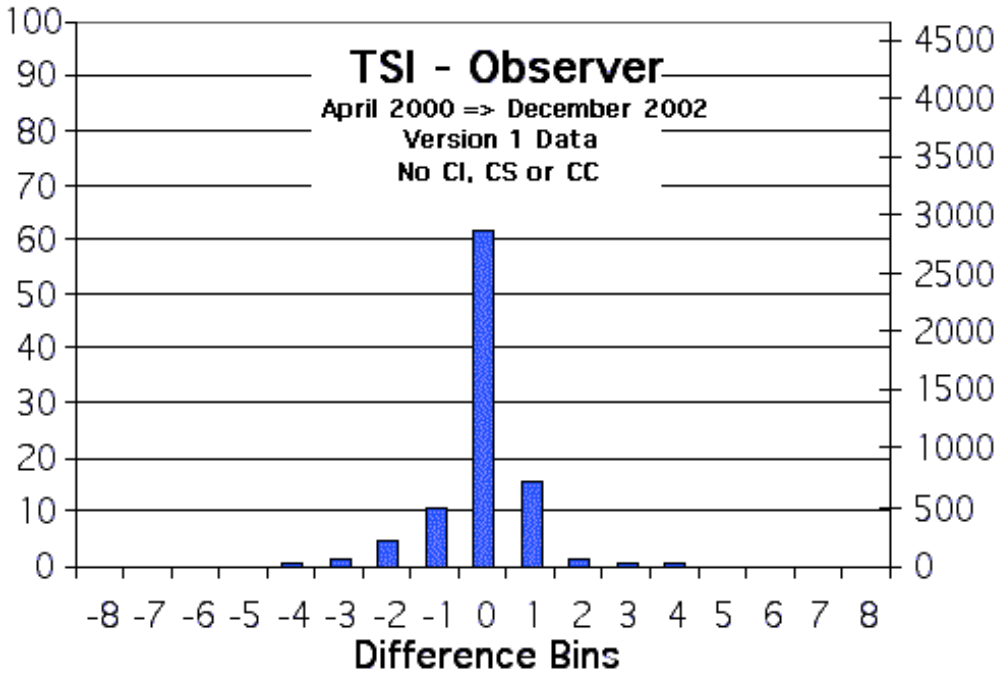

Figure 1 Difference between observer and TSI-derived cloud cover when only opaque clouds are present at the Desert Rock, Nev. SURFRAD station. The left ordinate is percent of the total, and the right ordinate is the number of comparisons.

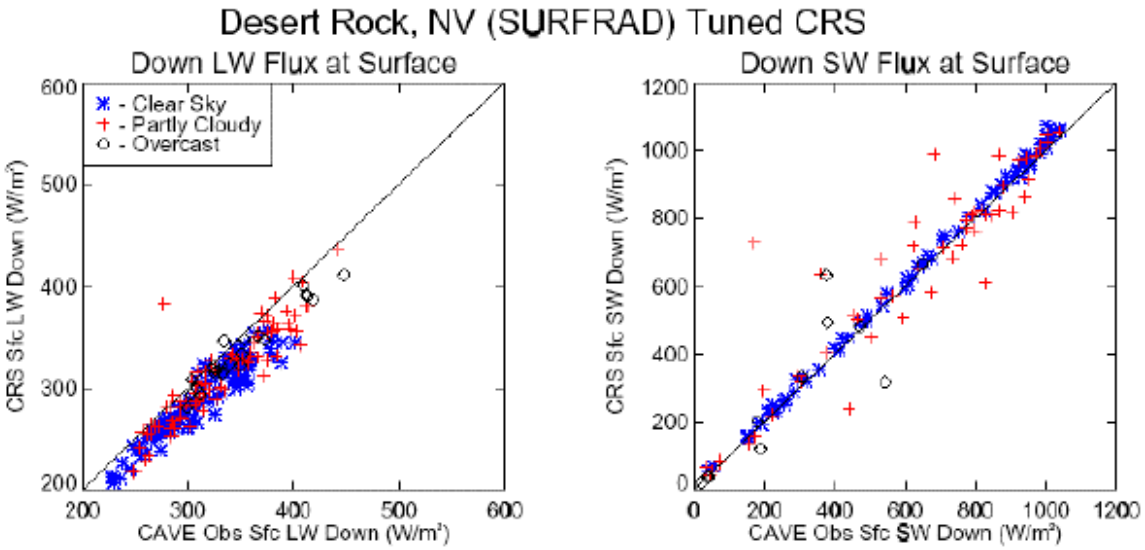

Figure 2. Sample validation plot of measured downwelling longwave (left) and shortwave (right) irradiance versus CERES-derived surface irradiance (represented on the abscissa) at the Desert Rock SURFRAD station for various sky conditions.

Provide SURFRAD data and specialized products to EOS investigators

All SURFRAD data were processed with the Long and Ackerman (2000) clear-sky software through March 2003 and the results were provided to NASA Langley for insertion into the CAVE archive and web site. An example of how SURFRAD data are used by EOS investigators is shown in Figure 2, which was retrieved from a NASA web site.

Investigate infrared cloud forcing

Long and Ackerman (2000) clear-sky calculations only provide objective measures of shortwave cloud forcing. However, to assess the complete radiative effect of clouds on the surface radiation budget, surface cloud forcing in the thermal infrared is also needed. An exploratory study was carried out to extend cloud forcing calculations to the infrared. This research involved finding a way to specify downwelling thermal infrared from a cloudless atmosphere. Theoretically, that may be computed using the following common relationship,

$$LW = \varepsilon * \sigma * T_a^4$$

where T_a is the air temperature, σ is the Stefan Boltzmann constant, and ε is the "effective emmisivity" of the atmosphere. The difficult part is specifying the effective atmospheric emmisivity because air does not behave as a black body. A formulation for the emmisivity of air was found in (Brutsaert 1975),

$$\varepsilon = 1.24 * (e / T_a)^{1/7}$$

This relationship is based on Schwarzschild's radiative transfer equation, where T_a and e are the near-surface air temperature and vapor pressure, respectively. The constant 1.24 is related to lapse rates of temperature and moisture, and was derived from an analysis of the standard atmosphere. Clear-sky downwelling thermal infrared irradiance was computed for clear-sky periods by applying the measured surface temperature and humidity to the equations listed above. Comparisons of these calculated values of downwelling infrared to SURFRAD downwelling infrared measurements showed an RMS error of 12.4 Wm^{-2}, a significant bias, and a $-33 Wm^{-2}$ offset.

Instead of using the generic value of 1.24, we improved this methodology by computing the lapse rate coefficient for each measurement time identified as clear by the Long and Ackerman shortwave clear-sky analysis. This was done by applying the surface temperature, humidity and downwelling infrared measurements of known clear-sky periods to the equations above, with the lapse rate coefficient as the unknown. The computed "clear sky" lapse rate coefficients were then used to calculate the effective emmisivity of the atmosphere for each of the clear-sky periods. In addition, the clear sky emmisivity was adjusted to include the effect of haze development for values of relative humidity greater than 75%. Clear-sky downwelling infrared calculations with the new emmisivities were then compared to downwelling infrared measurements (Figure 3). The RMS uncertainty was reduced by a factor of 2 over the results reported above (for which the generic value of 1.24 was used), and showed no significant bias or offset. The "clear-sky" lapse rate coefficients were interpolated for cloudy periods, thus producing a continuous string of calculated *clear-sky* downwelling thermal infrared. Subtracting the clear-sky thermal infrared estimates from SURFRAD downwelling thermal infrared measurements provided an objective estimate of longwave cloud forcing. This research is ongoing.

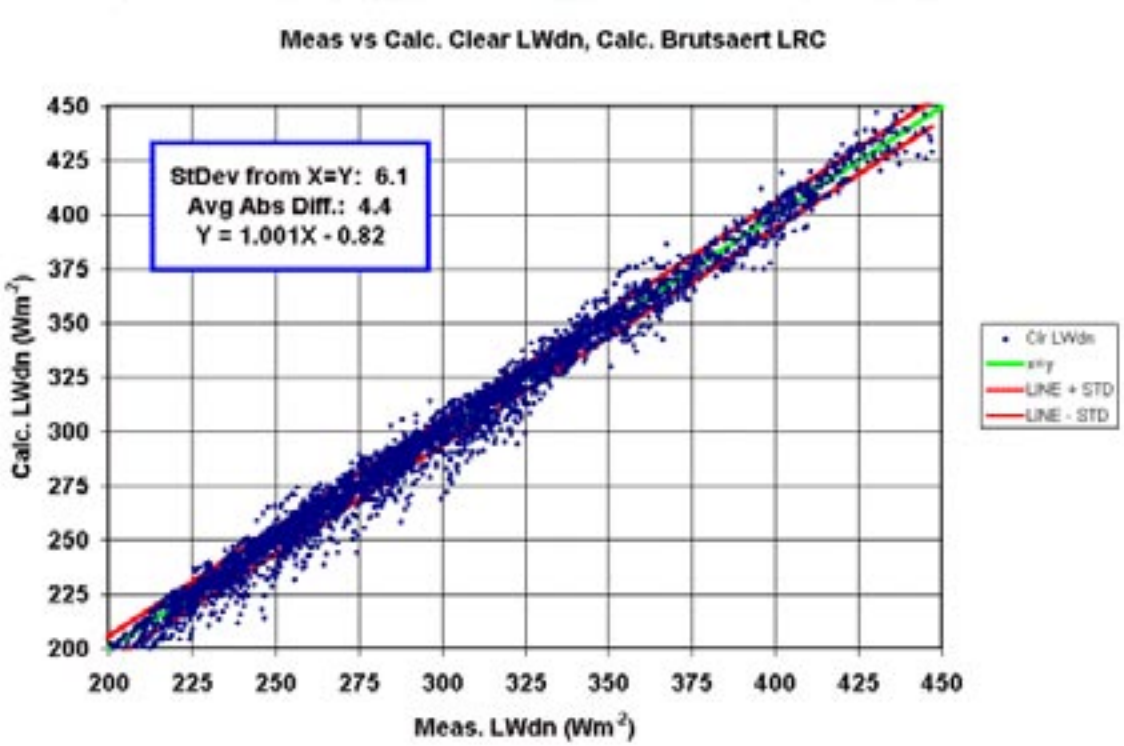

Figure 3. Clear-sky downwelling thermal infrared computed using an "effective emmisivity" of the air computed with our modified version of the Brutsaert (1975) formulation; versus measured downwelling thermal infrared at the ARM Southern Great Plains site.

Value of the interpolated soundings assessed radiatively

The purpose of providing interpolated soundings for SURFRAD station locations is to have profiles of temperature and moisture to initiate radiative transfer calculations. Therefore, a true test of the value of the interpolated soundings is to use them to initiate a radiative transfer model and compare the modeled downwelling thermal infrared to measured values. To do this we used RRTM model (Mlawer et al. 1997), which is a rapid and accurate model often used in climate and weather models.

The SURFRAD soundings were tested using RRTM for clear-sky conditions. The SURFRAD clear-sky products were used to identify clear periods at the 0000 and 1200 UTC synoptic times for all stations. Since the radiosonde balloons are typically launched an hour before the nominal synoptic time, and typically ascend for about an hour, the measured downwelling infrared data for the hour preceding the synoptic time were averaged. If that hour period was at least 75% clear it was included in the comparison.

Results for a one year period are shown in Figure 4 for the Fort Peck SURFRAD station. The comparisons of modeled and measured downwelling infrared are rather good, especially for periods with little variation in the surface measurement, as depicted by the error bars. When the measured downwelling infrared exhibits high variability during the hour averaging period, the modeled value shows a high bias. The cause of this degradation for times of high variability of the measured value is being investigated.

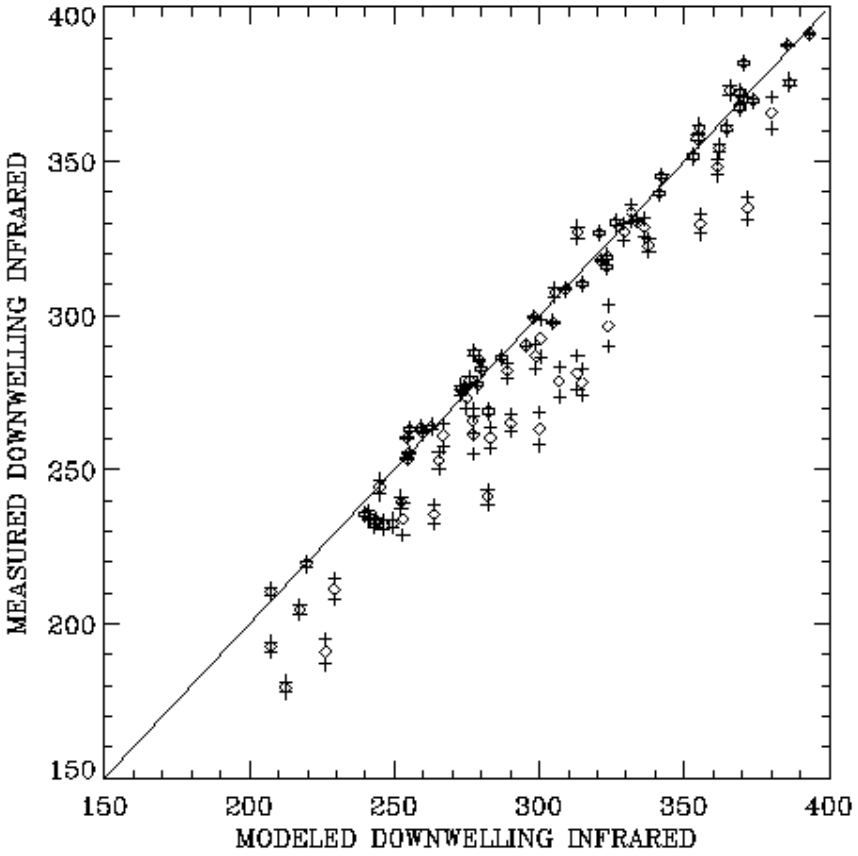

Figure 4. Measured versus modeled downwelling thermal infrared irradiance for the Fort Peck, MT SURFRAD station. Error bars represent the variation of the 3-min. downwelling infrared measurements during the hour-long balloon ascent time that the sounding data represents. A comparison was made only if 75% of the measurements during the hour were identified as clear.

MFRSR calibration and AOD analysis method improved

The method of MFRSR calibration and AOD analysis described in last year's progress report has been published (Augustine et al. 2003). The new method has also been completely automated and improved (Augustine and Medina 2003). The fully automated algorithm operates on a user-defined period of usually a month or two. First, the new algorithm matches MFRSR data times to periods of clear sky, as reported by the clear-sky analysis results. The algorithm then splits the clear-sky MFRSR data into morning and afternoon periods, and constructs a set of calibration Langley plots, which are displayed for inspection. Any anomalous calibration Langley plots may be removed at this point. Next, the algorithm applies linear regression to each calibration Langley plot. From those, a pool of I_0 intercepts is assembled, and a mean and standard deviation are computed. I_0 samples beyond one standard deviation from the mean are eliminated, and the remaining values are averaged to produce a more accurate calibration I_0 and standard error. This attempt to increase the accuracy of the ultimate I_0 calibration value was alluded to, but not applied in

Augustine et al. (2003). The resultant calibration I_0 is applied to individual MFRSR 500-nm measurements within the calibration period to compute the total optical depth. Contributions to the total optical depth from molecular scattering and ozone absorption are removed using methods reported in Augustine et al. (2003). Absorption by NO_2 is ignored because it was shown to be negligible for 500 nm measurements, even in cases of very high air pollution.

The first test of the completely automated method was to reprocess the period analyzed in Augustine et al. (2003). For that period (late March through late May 2001), the automated algorithm chose 15 periods that it deemed suitable for calibration Langley plots, whereas the semi-automated method used in Augustine et al. (2003) used 18. This discrepancy is explained by the practice of the automated method to reject measurements made for optical path lengths less than 1.5 and greater than 6, as recommended by Harrison and Michalsky (1994). The mean I_0 computed by the new automated version of 7.387 ±0.023 compares well to the value reported in Augustine et al. (2003) of 7.38 ±0.057, although the standard error was reduced by more than half by the new statistical elimination methodology. The greater accuracy reduced the reported range of AOD error range from ±0.01 - ±0.05 (in Augustine et al. 2003) to <±0.01 - ±0.02 (see Figure 5). The weighted averaging that was applied to the 18 calibration I_0 values in Augustine et al. (2003) was not applied in the automated method because, in all cases tested, there was little difference between the normal and weighted average.

For an independent test, the fully automated MFRSR calibration code was applied to Bondville MFRSR data for the month of October 2001. Bondville was chosen because the SURFRAD station there is collocated with an AERONET sun photometer (Holben et al. 2001). Of the fifteen extrapolated I_0 values, five were rejected because they were more than one standard deviation from the mean. The mean of the remaining values of 0.644 ± 0.021 represents the calibration I_0 for that month.

The computed calibration I_0 was applied to Bondville MFRSR 500-nm data for 3 October 2001. Results are shown in Figure 6. The AOD values are indicated by the green triangles; the horizontal bars represent the error bounds on the AOD values. Time is presented in UTC to facilitate comparison with AERONET results (Figure 7). Figure 6 shows that the trend in aerosol loading for that day is upward, with the lowest values of about 0.1 occurring in the early morning. The aerosol optical depth ramps up to a short-lived peak of >0.2 around noon (1800 UTC), then appears to settle to a mean value of about 0.17 for remainder of the afternoon, with intermittent spikes of short-lived higher values.

The AOD analysis of the Bondville AERONET sunphotometer 500 channel data in Figure 7 (green curve) shows a nearly identical time series as the MFRSR-based results in Figure 6. Given the similarity of these time series, the random nature of the comparison, and the fact that the MFRSR and AERONET instruments are quite different, offers encouragement that our automated method provides reliable AOD data. This new proven and automated method of AOD analysis presents opportunities for EOS investigators to use AOD data from SURFRAD stations for validation of MODIS aerosol products, and for use in testing the sensitivity of CERES algorithms to aerosols.

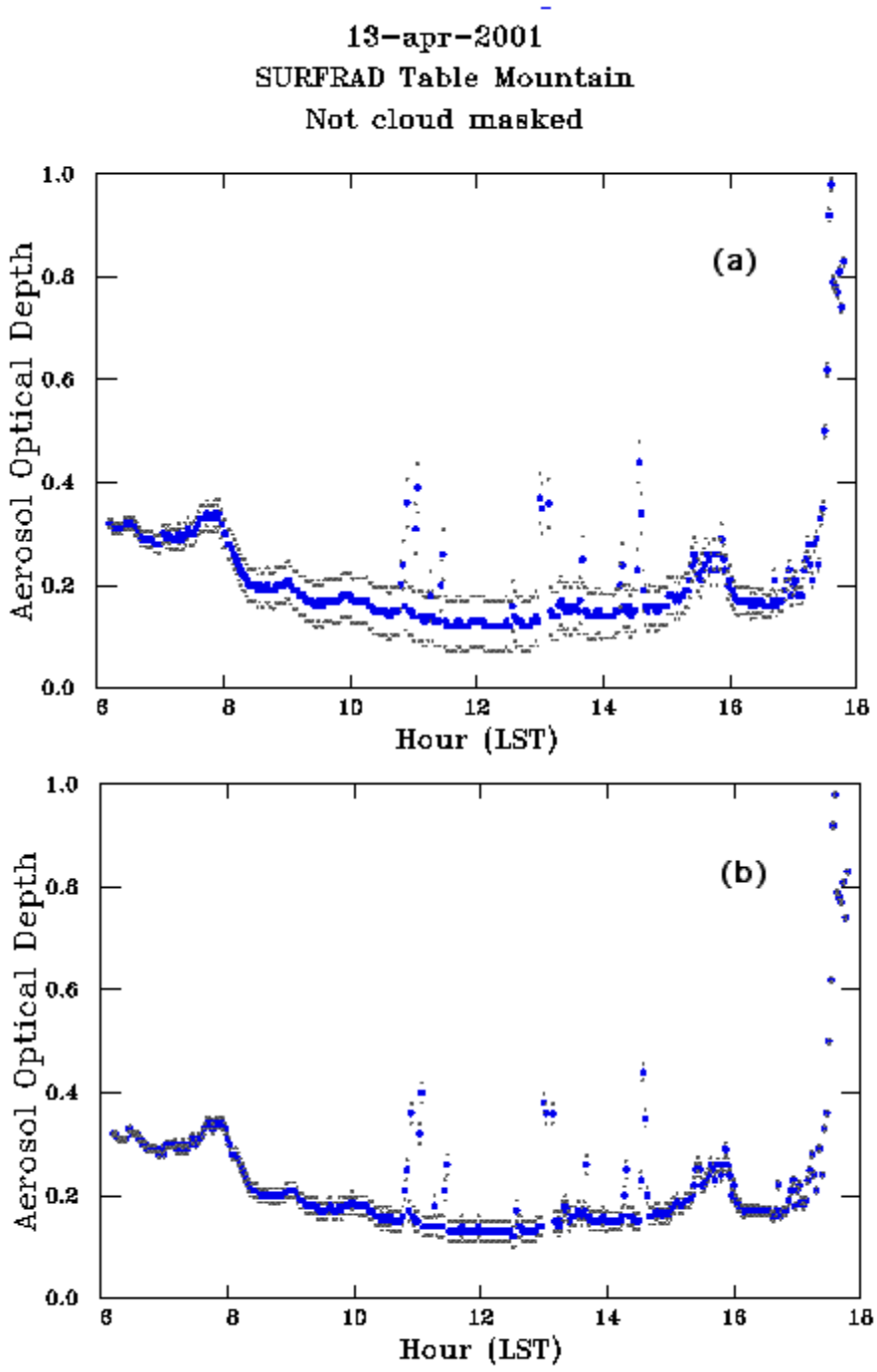

Figure 5. Aerosol optical depth time series for 13 April 2001(blue dots), with (a) error bars (gray) reported in Augustine et al. (2003), and (b) reduced error using the new more accurate method of I_0 selection. Spikes in the two plots represent times when clouds contaminated the MFRSR measurements and should be ignored.

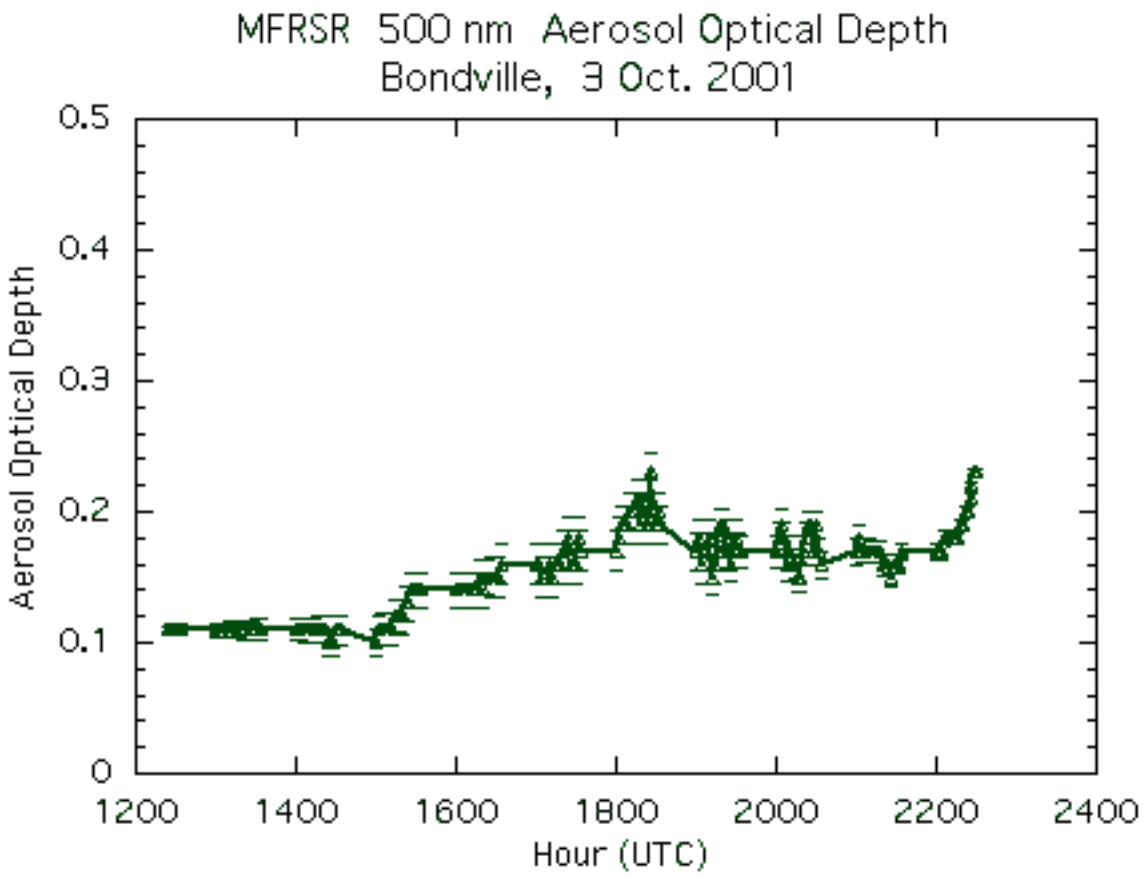

Figure 6. Aerosol optical depth time series at Bondville, Ill. for 3 October 2001 (green triangles), with error indicated by the horizontal lines above and below. These values were derived from MFRSR 500 nm data using the automated algorithm described in this paper.

Publications made possible through EOS validation funding

An article entitled "An automated method of MFRSR calibration for aerosol optical depth analysis with application to an Asian dust outbreak over the United States," was published in the February 2003 issue of the *Journal of Applied Meteorology*. Another paper entitled "A new automated method of MFRSR-based aerosol optical depth analysis" (Augustine and Medina 2003) was presented at the 12th Symposium on Meteorological Observations and Instrumentation, in Long Beach, CA, Feb. 10-14, 2003. The TSI cloud fraction validation effort reported here was also presented at the 12th Symposium on Meteorological Observations and Instrumentation in a paper by Gary Hodges entitled "A comparison of fractional cloud cover determinations by a sky imager with estimations by trained National Weather Service observers" (Hodges 2003).

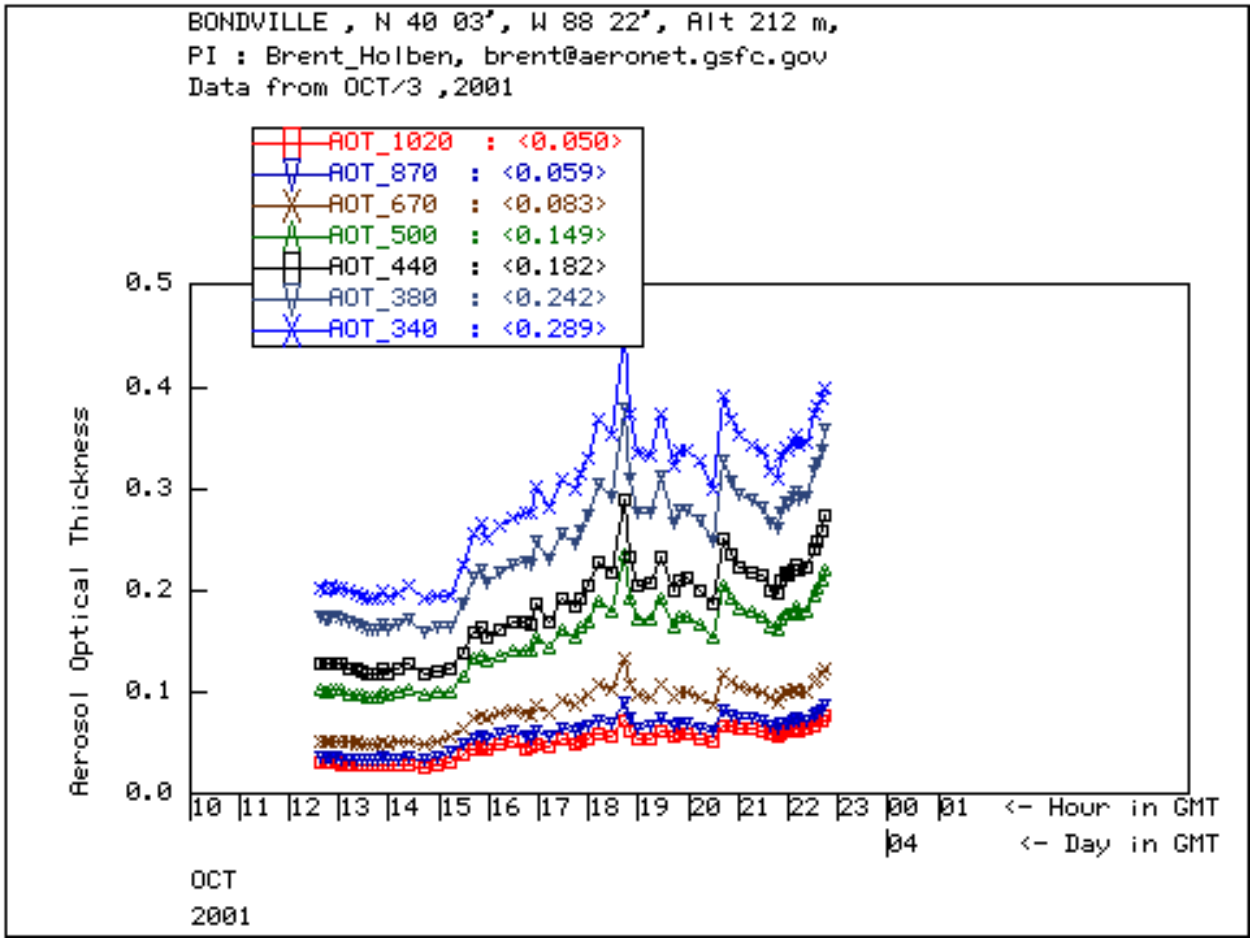

Figure 7. AERONET aerosol optical depth time series for Bondville, Ill. for 3 October 2001. The green triangles are AOD values derived from the 500-nm channel of the AERONET sunphotometer. This plot was obtained from the AERONET web site.

Planned activities

This was the final year of the present EOS validation contract. A proposal is currently in review from Ellsworth Dutton, John Augustine, Joe Michalsky, and Chuck Long in response to the NRA-03-OES-02 request for "Algorithm refinement" and validation proposals. The focus of the proposed work is to continue to provide surface radiation budget and other ancillary validation information to NASA from SURFRAD and the CMDL global networks.

References

Augustine, J. A., and C. I. Medina 2003: A new automated method of MFRSR-based aerosol optical depth analysis. *Proceedings, 12th Symposium on Meteorological Observations and Instrumentation*, February 9-13, 2003, Long Beach, Calif., CD

Augustine, J. A., C. R. Cornwall, G. B. Hodges, C. N. Long, C. I. Medina, and J. J. DeLuisi, 2003: An automated method of MFRSR calibration for aerosol optical depth

analysis with application to an Asian dust outbreak over the United States, *J. Appl. Meteor*., **42**, 266-278.

Brutsaert, W., 1975: On a Derivable Formula for Longwave Radiation from Clear Skies, *Water Resour. Res.*, **11**, 742-744.

Harrison, L, and J. Michalsky, 1994: Objective algorithms for the retrieval of optical depths from ground-based measurements. *Appl. Opt.*, **33**, 5126-5132.

Hodges, G., 2003: A comparison of fractional cloud cover determinations by a sky imager with estimations by trained National Weather Service observers. *Proceedings, 12th Symposium on Meteorological Observations and Instrumentation*, February 9-13, 2003, Long Beach, Calif., CD

Holben, B. N., D. Tanre, A Smirnov, T. F. Eck, I. Slutsker, N. Abuhassan, W. W. Newcomb, J. S. Schafer, B. Chatenet, F. Lavenu, Y. J. Kaufman, J. Vande Castle, A. Setzer, B. Markham, D. Clark, R. Frouin, R. Halthore, A. Karnieli, N. T. O'Neill, C. Pietras, R. T. Pinker, K. Voss, and G. Zibordi, 2001: An emerging ground-based aerosol climatology: Aerosol optical depth from AERONET. *J. Geophys. Res*., **106**, D11, 12067-12097.

Long, C. N. and T. P. Ackerman, 2000: Identification of Clear Skies from Broadband Pyranometer Measurements and Calculation of Downwelling Shortwave Cloud Effects, *J. Geophys. Res*., 105, D12, 15,609-15,626.

Mlawer, E. J., S. J. Taubman, P. D. Brown, M. J. Iacono, and S. A. Clough, 1997: Radiative transfer for inhomogeneous atmospheres: RRTM, a validated correlated-k model for the longwave, *J. Geophys. Res.*, **102**, D14, 16663-16682.